



Comparison of Human Erythrocyte Filterability with Trapping Rate Obtained by Nickel Mesh Filtration Technique: Two Independent Parameters of Erythrocyte Deformability

Takeshi Arita¹, Mitsuhiro Fukata¹, Toru Maruyama^{1*}, Keita Odashiro¹,
Takehiko Fujino², Chizuko Wakana², Aya Sato³, Kazue Takahashi³,
Yoshiko Iida³, Shiro Mawatari³ and Koichi Akashi¹

¹Department of Medicine, Kyushu University, Fukuoka 812-8582, Japan.

²BOOCS Clinic, Fukuoka 812-0025, Japan.

³Institute of Rheological Function of Foods Co., Ltd., Hisayama 811-2501, Japan.

Authors' contributions

This work was carried out in collaboration between all authors. Author TA performed main part of this research project. Author MF performed main part of manuscript preparation, and author TM supervised his manuscript preparation as a corresponding author. Author KO enrolled subjects and performed practical data extraction from medical records. Authors TF and CW had the initial concept of this research project and grew up the study protocol. Authors AS, KT and YI performed rheological experiments, and author SM supervised their experiments. Finally, author KA is a team leader and supervised the team collaboration. All authors read and approved the final manuscript.

Article Information

DOI: 10.9734/IBRR/2018/44667

Editor(s):

(1) Dr. Arnel Herve Nwabo Kamdje, Professor, Department of Biomedical Sciences, University of Ngaoundere, Cameroon.

Reviewers:

(1) Lian Zhao, Beijing Institute of Transfusion Medicine, China.

(2) Neema Tiwari, King George's Medical University, India.

Complete Peer review History: <http://www.sciencedomain.org/review-history/26744>

Original Research Article

Received 05 July 2018

Accepted 14 October 2018

Published 22 October 2018

ABSTRACT

Background: Erythrocyte deformability is a major determinant of microcirculation *in vivo*. Although this concept was defined as filterability evaluated by flow-pressure curve constructed during a filtration process of erythrocyte suspension through a nickel mesh filter, the behaviours of erythrocytes during the filtration process are unknown.

*Corresponding author: E-mail: maruyama@artsci.kyushu-u.ac.jp;

Aim: The present study aimed to obtain the better rheological understanding of the behaviours of erythrocytes passing through the nickel mesh filter.

Methods: Blood sample was obtained from 8 apparently healthy subjects after obtaining informed consent. Erythrocyte filterability (%) was calculated as the flow rate of a hematocrit-adjusted erythrocyte suspension relative to that of saline at a filtration pressure of 100 mmH₂O in flow-pressure curves obtained by nickel mesh filtration technique. Nickel mesh filters showing specific pore sizes of 6.00 µm (step 1) and 5.31 µm (step 2) were chosen, and two-step filtration protocol was performed. Erythrocytes counts (EC) were performed immediately before (EC_{pre}) and after (EC_{post}) each filtration, and erythrocyte trapping rate (%) was defined as $(EC_{pre} - EC_{post}) / EC_{pre}$. Erythrocyte filterability and trapping rate were correlated in each step for data analysis.

Results: EC_{pre} was always greater than corresponding EC_{post} in every subject and in both steps. Erythrocyte filterability in the step 1 ($91.8 \pm 2.1\%$) was close to that in the step 2 ($90.0 \pm 10.3\%$). Likely, the trapping rate in the step 1 ($77.8 \pm 2.4\%$) was close to that in the step 2 ($79.4 \pm 7.0\%$). Mean filterability in step 1 did not differ from that in step 2 ($p = 0.637$), and the same was true with respect to the mean trapping rate ($p = 0.516$). However, individual comparison between the filterability and the trapping rate of both steps demonstrated no correlation.

Conclusions: The present findings indicate that erythrocytes in suspension are trapped substantially by our nickel mesh filter. This trapping rate was not correlated to the erythrocyte filterability obtained by the flow-pressure curve during the nickel mesh filtration. Therefore, the erythrocyte trapping rate should be considered as a hemorheological parameter independent of the erythrocyte filterability.

Keywords: Deformability; erythrocytes; filtration; nickel mesh; trapping.

1. INTRODUCTION

The deformability of circulating erythrocytes is a major determinant affecting microcirculation *in vivo*. However, the concept of erythrocyte deformability has not been strictly defined as a physical quantity. Moreover, sensitivity, reproducibility and quantification of deformability measurement depend on the hemorheological techniques [1]. Erythrocyte deformation involves cellular bending within capillaries showing the minimum diameter less than an average diameter of erythrocytes. Therefore, bending deformability is defined as filterability, if filtration process of erythrocyte suspension is quantitative and reproducible. In our laboratory, deformability of human erythrocytes has been investigated by using a highly sensitive and quantitative nickel mesh filtration technique. Impairment of the deformability of erythrocytes obtained from patients with hypertension, diabetes and dyslipidemia was confirmed [2-6] and improvement of the deformability by therapeutic intervention was also observed [7]. However, the erythrocytes behaviours during the filtration process are unknown by this nickel mesh filtration technique, i.e., it is unclear whether all the erythrocytes are passed through the nickel mesh filter or a fraction of the erythrocytes is trapped by this filter. Because flow-pressure relationships obtained by the filtration of erythrocyte suspension pass through the origin, indicating that filtration is accomplished at the

zero filtration pressure [2,4,5]. Therefore, the present study was designed to obtain the better rheological understanding of the behaviors of erythrocytes passing through the nickel mesh filter.

2. MATERIALS AND METHODS

2.1 Study Location

Blood sampling of this study was performed at the BOOCS clinic (Fukuoka, Japan), Hemoheological investigation was conducted at the Institute of Rheological Function of Foods, Co., Ltd. (Hisayama, Japan), and data analyses and manuscript preparation was performed at the Department of Medicine, Kyushu University Hospital (Fukuoka, Japan).

2.2 Study Subjects

This study was performed according to the Declaration of Helsinki (2008) by enrolling apparently healthy subjects ($n = 8$) who visited the BOOCS clinic (Fukuoka, Japan) for health check. Signed informed consent was obtained from each subject prior to the enrollment in the study. Routine clinical examinations were performed. Laboratory data were extracted from medical records in a blind manner. The study design was approved by the internal ethics committee of the Institute of Rheological Function of Foods, Co., Ltd. (Hisayama, Japan).

2.3 Erythrocyte Suspension

Human erythrocyte suspensions were prepared as described elsewhere [2,5,7]. About 10 mL of venous blood was sampled from the antecubital vein of subjects ($n = 8$) after overnight fasting using 21-gauge needles and disposable syringes (Terumo Japan, Tokyo, Japan) filled with 1/10 volume of 3.8% trisodium citrate as an anticoagulant. After centrifugation at $1,300 \times g$ for 10 minutes, the supernatant was carefully aspirated to replace the buffy coat and plasma with saline buffered with N-(2-hydroxyethyl)-piperazine-N'-2-ethanesulfonic acid (HEPES) sodium salt (HEPES-Na). The composition of HEPES-Na-buffered saline (HBS) was NaCl 141 mM and HEPES-Na 10 mM. The osmolality and pH of the HBS were 287 mOsm/kg \cdot H₂O and 7.4, respectively. The osmolality of the HBS was measured using a freezing point depression type osmometer (Fiske Mark 3 Osmometer, Fiske Associates, MA, USA). Intact erythrocytes were then washed three times by repeated centrifugation at $800 \times g$, $600 \times g$, and $500 \times g$ for 10 minutes, respectively, to make final erythrocyte suspension for filtration experiment.

2.4 Nickel Mesh Filter

Fig. 1A shows a scanning electron microscopic photograph of a nickel mesh filter that was produced in accordance with our specifications by a photofabrication technique (Dainippon Printing Co., Ltd., Tokyo, Japan). We specified that this filter should have an outer diameter of 13 mm, a filtration area of 8 mm in inner diameter, a filter thickness of 11 μ m, an interpore distance of 35 μ m and a pore number of about 55,600 (Tsukasa Sokken Co., Ltd., Tokyo, Japan). The vertical and cylindrical pores were distributed regularly across the filter without coincidence or branching. The pore entrances exhibited round and smooth transition into the pore interior. Diameter is exactly identical in all the pores in a specific nickel mesh filter. Filters showing a specific pore diameter ranging from 2.90 to 6.00 μ m are available for selection depending on the suspension materials [4]. After repeated preliminary experiments to select an appropriate pore size, nickel mesh filters with respective pore diameters of 6.00 μ m (step 1) and 5.31 μ m (step 2) were used.

2.5 Erythrocyte Filterability

A filtration study was performed blindly using a nickel mesh filtration apparatus (Model NOBU-II,

Tsukasa Sokken Co., Ltd., Tokyo, Japan), as shown in Fig. 1B. In brief, the relation between hydrostatic pressure (P ; mmH₂O) and time (t ; sec) was obtained during continuous filtration according to gravity using a pressure transducer. P was transformed to the height of a meniscus in a vertical tube (h ; mm). The tangent of the h - t curve determined by drawing points corresponding to different heights gives the rate of fall of the meniscus (dh/dt). Thereafter, by multiplying dh/dt by the internal cross-sectional area of the vertical tube, the relation of flow rates (Q ; mL/min) and corresponding P (P - Q curve) was obtained [6,7]. This procedure was automatically performed by measurement software installed on a personal computer (DELL Latitude CS, Dell Inc., Round Rock, TX, USA) and monitored on the main window of the computer screen. Together with the start of data acquisition, the measurement software displays the real-time h - t curve continuously during the filtration process. When filtration has been completed, the software displays the P - Q curve. The h - t and P - Q curves are stored simultaneously in Microsoft Office Excel 2003 on Windows XP (Microsoft, Tokyo, Japan). The temperature of the specimens was kept at 25°C by circulating isothermal water through a water jacket surrounding the vertical tube (Fig. 1B). The flow rate of the erythrocyte suspension as a percentage of that of HBS at 100 mmH₂O was used as an index of erythrocyte deformability. These experiments were performed at room temperature (22 ± 3 °C).

2.6 Erythrocyte Trapping Rate

Erythrocyte counting (EC) and hematocrit (Ht) measurement were performed in each step of preparation of the final suspension used for the following filtration experiment. The final Ht of the erythrocyte suspension was adjusted to 2.0%. EC was performed immediately before (EC_{pre}) and after (EC_{post}) the filtration study. Confirming that EC_{pre} was always greater than EC_{post} , difference of EC produced by the filtration process was considered to be based on the numbers of erythrocytes trapped by the nickel mesh *per se* during the filtration process. Therefore, trapping rate of erythrocytes was defined as follows;

$$\text{Trapping Rate} = (EC_{pre} - EC_{post}) / EC_{pre} (\%)$$

Blood cell counting and Ht measurement were performed using a hemocytometer (Ace Counter, FLC-240A, Fukuda Denshi Co., Ltd., Tokyo,

Japan). These procedures were performed within 2 hours after blood sampling.

2.7 Study Protocols

Erythrocyte suspension with a Ht of 2.0% were prepared, and EC_{pre} was obtained. First filtration experiment was performed using a nickel mesh filter with a pore size of 6.00 μm , and erythrocyte filterability was evaluated. Postfiltration suspension was harvested and trapping rate was calculated after obtaining EC_{post} (step 1). Erythrocyte suspension used in the step 1 was diluted by HBS to the final condition where EC_{pre} was adjusted to 9×10^4 / μl . Finally, filtration experiment using a nickel mesh filter with a pore size of 5.31 μm was performed using this erythrocyte suspension. Erythrocyte filterability was estimated and trapping rate was calculated after obtaining EC_{post} (step 2).

2.8 Data Analysis

All data are expressed as means \pm SD. For statistical analyses, Kolmogorov-Smirnov test was used first for normality, and test for independence was applied to seek independence of data distribution. To analyse the difference of the corresponding two steps, comparison of normally distributed continuous variables was conducted with paired Student's *t* test, and that of other variables was performed by the Wilcoxon's sign rank test. Multiple correlations were performed by Pearson's analysis when data showed normality and by Spearman's analysis when data did not show normality. These analyses were performed using Bell Curve for Excels version 2.12 (Social Survey Research Information Co., Ltd., Tokyo, Japan). Differences with two-sided $p < 0.05$ were considered significant.

3. RESULTS

Erythrocyte numbers in suspension with a Ht of just 2.0% prior to the step 1 filtration (EC_{pre}) ranged from 32×10^4 μl to 39×10^4 μl ($34.9 \pm 2.5 \times 10^4$ μl , $n = 8$), whereas EC_{post} in step 1 ranged from 24×10^4 μl to 30×10^4 μl ($27.1 \pm 2.0 \times 10^4$ μl , $n = 8$). With respect to the step 2 filtration, EC_{pre} was adjusted to 9×10^4 / μl , and EC_{post} ranged from 6×10^4 μl to 8×10^4 μl ($7.1 \pm 0.6 \times 10^4$ μl , $n = 8$). EC_{pre} was greater than corresponding EC_{post} in every subject and in both steps. Therefore, erythrocyte trapping rate ranged from 73% to 81% ($77.8 \pm 2.4\%$) in the step 1 filtration and from 67% to 89% ($79.4 \pm 7.0\%$) in the step 2

filtration. Trapping rate in the step 1 showed normality, whereas that in the step 2 did not show normality. Mean trapping rate in the step 1 did not differ from that in the step 2 ($p = 0.516$).

Representative flow-pressure curves obtained by nickel mesh filtration technique in the step 2 were presented in Fig. 2. Flow-pressure relationships obtained by HBS filtration showed straight line passing through the origin, whereas the relationships obtained by the filtration of erythrocyte suspensions displayed smooth curves convex to abscissa and passed through the origin. These confirm that cell-free medium (i.e., HBS) is Newtonian fluid and erythrocytes-suspending medium is not Newtonian fluid. Filterability calculated by these curves yielded 86.2%, 83.8% and 82.4% in the respective three subjects enrolled. Erythrocyte filterability evaluated in the step 1 ranged from 88% to 93% ($91.8 \pm 2.1\%$, $n = 8$), whereas that in the stage 2 scattered from 65% to 96% ($90.0 \pm 10.3\%$, $n = 8$). Filterability in the step 1 showed normality, whereas that in the step 2 did not show normality. Mean filterability in the step 1 did not differ from that in the step 2 ($p = 0.637$).

Individual filterability and trapping rate of two steps were demonstrated in Fig. 3. Spearman's comparison between the filterability and the trapping rate of both steps demonstrated no significant correlations, and test for independence revealed no dependence at all among the four parameters (Cramer's $V = 0.032$, $p = 0.995$).

4. DISCUSSION

4.1 Main Findings

The main findings of this study using the sensitive, reproducible, and quantitative nickel mesh filtration technique (Fig. 1) are that significant numbers of erythrocytes are trapped by this nickel mesh filter during filtration process, that erythrocyte filterability are not correlated with erythrocyte trapping rate, and hence that the trapping rate should be considered as an independent rheological parameter of erythrocytes aside from the filterability.

4.2 Hematocrit Adjustment

In our preliminary experiments, Ht was titrated to realise sensitive and reproducible filtration of erythrocyte suspension. For this purpose, nickel mesh filter was sonicated after each filtration

experiment to prevent filter fouling. Complete cleansing of nickel mesh filter was confirmed by filtration of HBS and obtaining the linear flow-pressure relation which was completely superimposed with the previous linearity of HBS filtration, because this linearity is compatible to the Newtonian behavior of HBS. This sonication depends on Ht of the erythrocyte suspension, i.e., the greater Ht required the longer sonication time. Finally, Ht of erythrocyte suspension was adjusted to 2-3% depending on the species (human or rats) [2, 4]. This low Ht was supposed to allow the measurement of filterability in all the erythrocytes without aggregation [8], although erythrocytes behaviors during filtration process were not clear.

4.3 Microstructure of Nickel Mesh Filter

The sensitivity and the reproducibility of the filtration technique depend on the microstructure of the filter. Material of the filter is nickel, resistant to repetitive sonication, which is essential to avoid membrane fouling. This filter shows completely regular distribution of numerous pores with their uniform diameter (Fig. 1A). The pores have no branching and no coincidence across the filter. Moreover, the pore entrance shows round and smooth transition into the inside, i.e., tapering of pore entrance prevents

mechanical activations of leukocytes or platelets contaminated in the erythrocyte suspension, if any. This tapering is considered to prevent the mechanical damage on erythrocytes and to promote smooth bending deformation of erythrocytes going into the filter inside. Our colleagues investigated the correlation between the pore size measured by scanning electron microscopic (SEM) examination (y) and the pore size calculated by Hagen-Poiseuille's law applied to the flow-pressure relationship obtained by clean air flowing through the nickel mesh filter (x). They obtained the regression equation of $y = 0.94x - 0.74$ [9].

This comparative investigation demonstrates highly linear regression ($r^2 = 0.98$, $p = 0.0001$) between the SEM-measured pore size (y) and aerodynamically calculated pore size (x). Moreover, this study indicates that the former is always smaller than the latter, i.e., SEM observation allows the measurement of minimum size of pores at the middle depth of the nickel mesh filter, whereas aerodynamic calculation reflects smooth tapering around the pore entrance at the surface of the filter, which has significant rheological impact on the natural and fluent erythrocyte filtration process, allowing smooth bending of erythrocytes entering the pore inside.

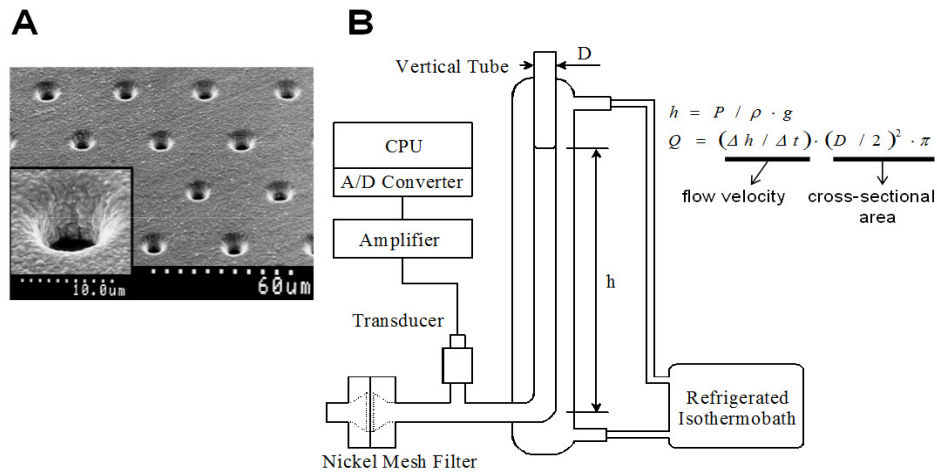


Fig. 1. A: Scanning electron microscopic (SEM) photograph of a nickel mesh filter. Magnification of a single pore in the nickel mesh shows the smooth transition into the pore interior (inset). B: Schematic illustration of the nickel mesh filtration system. The two equations indicate how to calculate the relationship between the flow rate (Q) and filtration pressure (P). The height of the meniscus (h) within the vertical tube was obtained by the continuous reduction of P during the filtration, specific gravity of the specimens within the tube (ρ), and acceleration of gravity (g). Q was calculated automatically by the first time derivative of h (dh/dt) and internal cross-sectional area of the tube (D , internal diameter of the vertical tube). The obtained P - Q relationship is displayed on the computer screen.

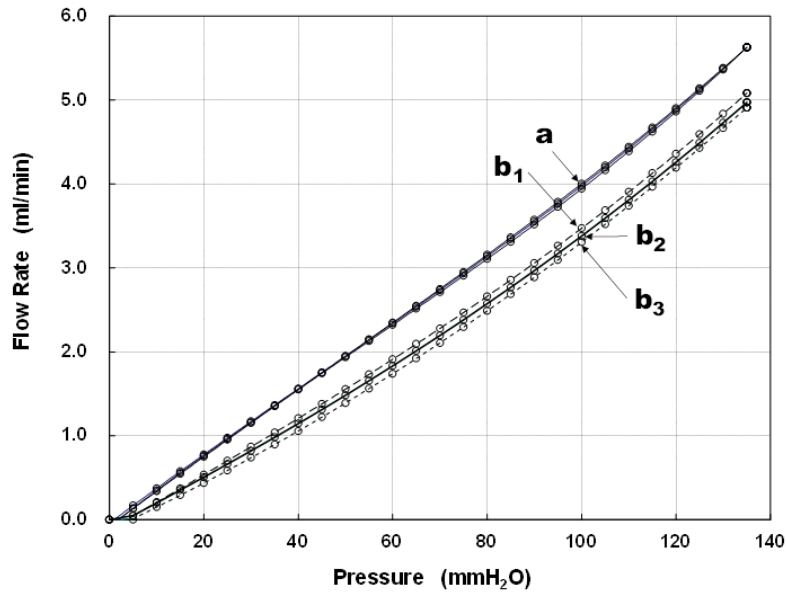


Fig. 2. Pressure-flow curves obtained by nickel mesh filtration technique at the step 2. Filtration of HEPES-buffered saline (HBS) yielded linear pressure-flow relationship, whereas the filtration of erythrocyte suspensions obtained by three different subjects showed curves convex to abscissa. Filterability is calculated by flow rate (ml/min) of erythrocyte suspension divided by that of HBS at the filtration pressure of 100 mmH₂O (b_1/a , b_2/a and b_3/a). Note that flow rate of erythrocyte suspension is always lower than that of HBS at any filtration pressure, and that linearity of HBS is superimposable indicating the reproducibility of this filtration system.

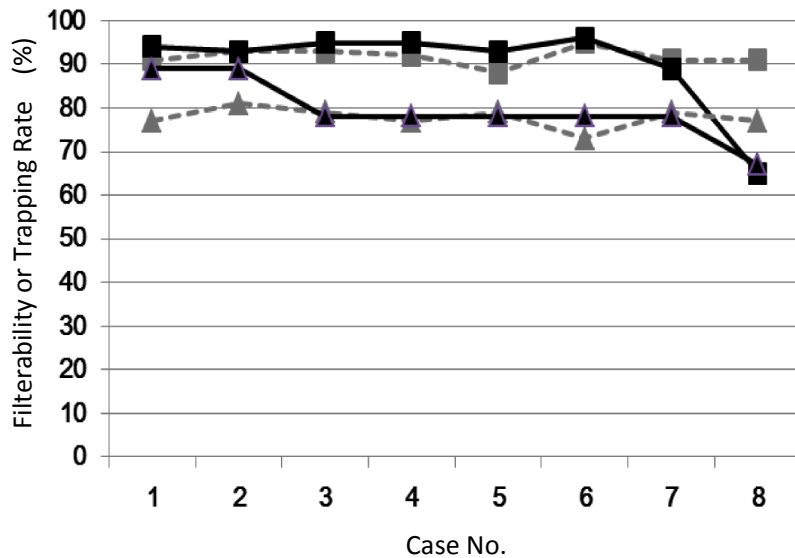


Fig. 3. Erythrocyte filterability (%) in the step 1 (■) and 2 (▲) and erythrocyte trapping rate (%) in the step 1 (□) and 2 (△) of all the enrolled subjects (n = 8) are indicated. No specific correlation between the two steps were found, and the filterability was independent from trapping rate.

4.4 Comparison of Filterability with Trapping Rate

So far, in our laboratory, erythrocyte deformability was considered as filterability (%) defined as a flow rate of erythrocyte suspension divided by a flow rate of HBS at 100 mmH₂O (Fig. 2). In this filtration process, we have no guarantee concerning whether all the erythrocytes in suspension passed through the numerous narrow pores or not. In the present study, we found that approximately 20% of erythrocytes in suspension (Ht of 2.0%) were trapped by a nickel mesh filter pores, which is independent of the pore size (Fig. 3).

Erythrocyte suspension contains numerous erythrocytes with various stages of aging up to 120 days. Circulating mature erythrocytes are gradually aging, and intravascular mechanical, osmotic or oxidative stress declines ATP production based on erythrocyte membrane glycolysis. These stresses cause intracellular Ca²⁺ accumulation associated with PIEZO1 and Gardos channel appearance [10] leading to cellular dehydration [11], decreased membrane fluidity [12 - 14] and impairment of deformability [15 - 17]. Trapped erythrocytes are assumed to be the population containing aged, damaged or dehydrated erythrocytes. On the other hand, erythrocyte filterability is based on the flow-pressure curve of erythrocyte suspension obtained by filtration process. Filterability of erythrocytes reflects the population of erythrocytes passing through the nickel mesh filter. Therefore, filterability reflects the erythrocyte population which differs from the population reflected by trapping rate.

There have been several investigations reporting that circulating erythrocytes *in vivo* are trapped selectively by organs damaged by ischemia-reperfusion insults [18] and that adhesive or dense erythrocytes (such as sickle cells) are trapped by intact vascular endothelium leading to thrombus formation [19]. These pathological phenomena lead to vascular occlusion and damaged organ congestion. It is of importance that our two-step protocol demonstrated that the filterability and trapping rate in the first step (pore diameter of 6.00 μm) showed normality, whereas those in the second step (pore diameter of 5.31 μm) did not show normality. These indicate 1) that dense or aged erythrocytes are present as a fraction of erythrocytes population and trapped by the two step filtration system, and 2) that pore size of 5.31 μm is critical for damaged

erythrocytes to pass through the filter. This may be supported by our observation that standard deviations of both mean filterability and trapping rate in the second step were larger than those in the first step.

5. CONCLUSIONS

Although this is a small-sample study and should be applied to patients showing microcirculatory disturbance such as hypertension, diabetes or dyslipidemia, this study demonstrated that a fraction of erythrocytes in suspension are trapped by the nickel mesh filters during the process of filtration according to the gravity in apparently healthy subjects. The nickel mesh filters show a regular distribution of uniform pores with identical diameter less than average diameter of human erythrocytes. The trapping rate was calculated by erythrocytes counts immediately before and after the filtration. The trapping rate was not correlated to the erythrocyte filterability obtained by the flow-pressure curve during the filtration. Therefore, the erythrocyte trapping rate should be considered as a hemorheological parameter independent of the erythrocyte filterability.

CONSENT

Medical information extraction was informed to and signed informed consent was obtained from all the subjects at the enrollment.

ETHICAL APPROVAL

All the procedure performed in this study were in accordance with the ethical standards of our institutional and/or national research committee and with updated Declaration of Helsinki (2008).

COMPETING INTERESTS

Authors have declared that no competing interests exist.

REFERENCES

1. Mohandas N, Chasis JA. Red cell deformability, membrane material properties and shape: regulation by transmembrane, skeletal and cytosolic proteins and lipids. *Semin Hematol.* 1993; 30(3):171-192.
2. Saito K, Kogawa Y, Fukata M, Odashiro K, Maruyama T, Akashi K, Fujino T. Impaired

- deformability of erythrocytes in diabetic rat and human: investigation by the nickel-mesh-filtration technique. *J Biorheol.* 2011; 25(1-2):18-26.
3. Iwata H, Ukeda H, Maruyama T, Fujino T, Sawamura M. Effect of carbonyl compounds on red blood cells deformability. *Biochem Biophys Res Comm.* 2004;321(3):700-706.
 4. Ariyoshi K, Maruyama T, Odashiro K, Akashi K, Fujino T, Uyesaka N. Impaired erythrocyte filterability of spontaneously hypertensive rats: Investigation by nickel mesh filtration technique. *Circ J.* 2010;74(1):129-136.
 5. Odashiro K, Saito K, Arita T, Maruyama T, Fujino T, Akashi K. Impaired deformability of circulating erythrocytes obtained from nondiabetic hypertensive patients: Investigation by a nickel mesh filtration technique. *Clin Hypertens.* 2015;21:17.
 6. Ejima J, Ijichi T, Ohnishi Y, Maruyama T, Kaji Y, Kanaya S, Fujino T, Uyesaka N, Ohmura T. Relationship of high-density lipoprotein cholesterol and red blood cell filterability: cross-sectional study of healthy subjects. *Clin Hemorheol Microcirc.* 2000; 22(1):1-7.
 7. Saito K, Odashiro K, Maruyama T, Akashi K, Mawatari S, Fujino T. Improvement of diabetic or obese patients' erythrocyte deformability by the program of the brain-oriented obesity control system (BOOCS). *J Physiol Sci.* 2012;62(6):445-451.
 8. Arbell D, Orkin B, Bar-Oz B, Barshtein G, Yedgar S. Premature red blood cells have decreased aggregation and enhanced aggregability. *J Physiol Sci.* 2008;58(3): 161-165.
 9. Uyesaka N, Yamawaki S, Oonishi T, Ishi Y, Kawa T, Shio H, Fujino T. Rheologic characterization of a porous thin metal filter and red cell deformability. *ICOM'96 Proceedings.* 1996;705.
 10. Lew VL, Tiffert T. On the mechanism of human red blood cell longevity: roles of calcium, the sodium pump, PIEZO1, and Gardos channels. *Front Physiol.* 2017;8: 977. DOI:10.3389/fphys.2017.00977. eCollection 2017.
 11. Gallagher PG. Disorders of erythrocyte hydration. *Blood.* 2017;130(25):2699-2708.
 12. Liu F, Mizukami H, Sarnaik S, Ostafin A. Calcium-dependent human erythrocyte cytoskeleton stability analysis through atomic force microscopy. *J Struct Biol.* 2005;150:200-210.
 13. Luneva OG, Brazhe NA, Maksimova NV, Rodnenkov OV, Parshina EY, Bryzgalova NY. Ion transport, membrane fluidity and haemoglobin conformation in erythrocyte from patients with cardiovascular diseases: role of augmented plasma cholesterol. *Pathophysiology.* 2007;14(1):41-46.
 14. Pytel E, Olszewska-Banaszczyk M, Koter-Michalak M, Broncel M. Increased oxidative stress and decreased membrane fluidity in erythrocytes of CAD patents. *Biochem Cell Biol.* 2013;91(5):315-318.
 15. Oonishi T, Sakashita K, Uyesaka N. Regulation of red blood cell filterability by Ca²⁺ influx and cAMP-mediated signaling pathways. *Am J Physiol.* 1997;273(6): C1828-C1834.
 16. Okamoto K, Maruyama T, Kaji Y, Harada M, Mawatari S, Fujino T, et al. Verapamil prevents impairment in filterability of human erythrocytes exposed to oxidative stress. *Jpn J Physiol.* 2004;54(1):39-46.
 17. Uyesaka N, Hasegawa S, Ishioka N, Ishioka R, Shio H, Schechter AN. Effects of superoxide anions on red cell deformability and membrane proteins. *Biorheology.* 1992;29(2-3):217-229.
 18. Wolf M, Drubbel V, Hendriks JM, Van Schil PE. Red blood cell accumulation in a rat model of pulmonary ischemia/reperfusion injury. *J Cardiovasc Surg.* 2009;50(3):351-356.
 19. Kaul DK, Fabry ME. In vivo studies of sickle red blood cells. *Microcirculation.* 2004;11(2):153-165.

© 2018 Arita et al.; This is an Open Access article distributed under the terms of the Creative Commons Attribution License (<http://creativecommons.org/licenses/by/4.0>), which permits unrestricted use, distribution, and reproduction in any medium, provided the original work is properly cited.

Peer-review history:

The peer review history for this paper can be accessed here:
<http://www.sciencedomain.org/review-history/26744>